American Journal of Electrical Power and Energy Systems
2013; 2(4): 98-105
Published online July 10, 2013 (http://www.sciencepublishinggroup.com/j/epes)
doi: 10.11648/j.epes.20130204.11

Enhancement of power system stability using self-organized neuro–fuzzy based HVDC controls

Nagu Bhookya, RamanaRao P. V, Sydulu Maheshwarapu

Department of Electrical and Electronics Engineering, National Institute of Technology Warangal, Andhra Pradesh, India

Email address:
nagu.research@gmail.com(N. Bhookya), ramana@nitw.ac.in(Ramanarao P. V), sydulumaheswarapu@yahoo.co.in(S. Maheshwarapu)

To cite this article:
Nagu Bhookya, RamanaRao P. V, Sydulu Maheshwarapu. Enhancement of Power System Stability Using Self-Organized Neuro–Fuzzy Based HVDC Controls. *American Journal of Electrical Power and Energy Systems*. Vol. 2, No. 4, 2013, pp. 98-105.
doi: 10.11648/j.epes.20130204.11

Abstract: This paper presents an affective neuro – fuzzy controller (NFC) to improve the transient stability of multi-machine system with HVDC link. Fuzzy rules are used as neurons in artificial neural network (ANN) model. Excellent learning capability of ANN and heuristic fuzzy rules and input/output membership functions of fuzzy logic technique are optimally tuned from training examples by back propagation algorithm (BPA). Considerable time required for fuzzy inference system to match rules is saved using NFC. To illustrate the performance of NFC, transient stability study is carried out on a multi machine system and results are compared with conventional controller as well as fuzzy logic controller.

Keywords: Neuro – Fuzzy Controller, Artificial Neural Network, Transient Stability, Back Propagation Algorithm

1. Introduction

HVDC power transmission system offers several advantages, one of which is rapid control of the transmitted power. Therefore, they have a significant impact on the stability of the associated AC power systems. Moreover, HVDC link effectively uses frequency control and improves the stability of the system using fast load-flow control. The importance of AC-DC power transmission systems in the improvement of stability has been a subject to much research. An HVDC transmission link is highly controllable. It is possible to take advantage of this unique characteristic of the HVDC link to augment the transient stability of the ac systems. In the past, numerous investigations have been carried out to improve transient stability of power system, ranging from theoretical studies to advanced control devices [1-4].

A proper design of the HVDC controls is essential to ensure satisfactory performance of overall AC/DC system [5-6]. The control strategy, traditionally employed for a two-terminal HVDC transmission system is the current margin method, where the rectifier is in current control, and the inverter is in constant extinction angle (CEA) control [4]. Both ends of the dc system rely on PI controllers to provide fast robust control. The conventional methods often require a precise mathematical model of the controlled system. Because of fixed gains (Kp, Ki, Kd) these controllers perform well over a limited operating range as for power systems in practice, there exists parameter uncertainty in plant modeling and large variations in environmental conditions. Therefore HVDC systems are prone to repetitive commutation failure when connected to a weak AC systems and also when subjected to faults and disturbances. This leads to considerable research in the field of effective control of HVDC systems using adaptive, optimal, intelligent controllers such as neural network, fuzzy logic,neuro – fuzzy controllers etc.

Artificial neural networks and fuzzy logic systems are successfully implemented for improvement of transient stability of power system [7]. The salient features of both techniques are combined to form a hybrid controller i.e. Neuro – fuzzy controller. Self-learning capability of neural network is combined with inference system of fuzzy logic to form self-organizing neuro – fuzzy controller. Thus in this paper, the feasibility of employing a neuro – fuzzy controller for an HVDC transmission system is explored. To demonstrate the effectiveness of proposed NFC, NFC is employed to improve transient stability of a WSCC 9 bus system and the response of the NFC is compared with conventional controller.

2. AC/DC Load Flow Analysis

In transient stability studies it is a prerequisite to do AC/DC load flow calculations in order to obtain system conditions prior to the disturbance [5]. While the conventional approaches are available for conducting the calculations, the eliminated variable method proposed by Anderson, et al[8] is used here which treats the real and reactive powers consumed by the converters as voltage dependent loads. The dc equations are solved analytically or numerically and the dc variables are eliminated from the power flow equations. The method is however unified in the sense that the effect of the dc – link is included in the Jacobian matrix.

2.1. DC System Model

The equations describing the steady state behavior of a mono polar DC link can be summarized as follows [9],

$$V_{dr} = \frac{3\sqrt{2}}{\pi} a_r V_{tr} \cos\alpha_r - \frac{3}{\pi} X_c I_d \quad (1)$$

$$V_{di} = \frac{3\sqrt{2}}{\pi} a_i V_{ti} \cos\gamma_i - \frac{3}{\pi} X_c I_d \quad (2)$$

$$V_{dr} = V_{di} + r_d I_d \quad (3)$$

$$P_{dr} = V_{dr} I_d \quad (4)$$

$$P_{di} = V_{di} I_d \quad (5)$$

$$S_{dr} = k \frac{3\sqrt{2}}{\pi} a_r V_{tr} I_d \quad (6)$$

$$S_{di} = k \frac{3\sqrt{2}}{\pi} a_i V_{ti} I_{d0} \quad (7)$$

$$Q_{dr} = \sqrt{S_{dr}^2 - P_{dr}^2} \quad (8)$$

$$Q_{di} = \sqrt{S_{di}^2 - P_{di}^2} \quad (9)$$

Where,

Vdr, Vdi	voltages at rectifier and inverter end respectively
Vtr, Vti	terminal voltages at rectifier and inverter ends
Id	dc link current
Xc, rd	dc link reactance and resistance
α, □	firing and extinction angle respectively
a	tap ratio
Pdr, Pdi	Real power at rectifier and inverter ends resp.
Qdr,Qdi	Reactive power at rectifier and inverter ends resp.
Sdr, Sdi	Apparent power at rectifier and inverter ends resp.

2.2. The Eliminated Variable Method

The real and reactive powers consumed by the converters are expressed as function of their ac terminal voltages, Vtr and Vti. Their partial derivatives with respect to Vtr and Vti are computed and used in modification of Jacobian elements of the Newton Raphson power flow solution as shown below,

$$\begin{bmatrix} \frac{\Delta P}{\Delta Q} \end{bmatrix} = \begin{bmatrix} H & N \\ M & L \end{bmatrix} \begin{bmatrix} \frac{\Delta \delta}{\Delta V / V} \end{bmatrix} \quad (10)$$

$$N'(tr,tr) = V_{tr} \frac{\partial P_{tr}^{ac}}{\partial V_{tr}} + V_{tr} \frac{\partial P_{dr}(V_{tr},V_{ti})}{\partial V_{tr}} \quad (11)$$

$$N'(tr,ti) = V_{ti} \frac{\partial P_{tr}^{ac}}{\partial V_{ti}} + V_{ti} \frac{\partial P_{dr}(V_{tr},V_{ti})}{\partial V_{ti}} \quad (12)$$

$$N'(ti,tr) = V_{tr} \frac{\partial P_{tr}^{ac}}{\partial V_{tr}} - V_{tr} \frac{\partial P_{di}(V_{tr},V_{ti})}{\partial V_{tr}} \quad (13)$$

$$N'(ti,ti) = V_{ti} \frac{\partial P_{tr}^{ac}}{\partial V_{tr}} - V_{ti} \frac{\partial P_{di}(V_{tr},V_{ti})}{\partial V_{ti}} \quad (14)$$

L' is also modified analogously. Thus, in the eliminated variable method, four mismatch equations and up to eight elements of Jacobian have to be modified, but no new variables are added to solution vector, when a dc – link is included in the power flow.

3. Representation of HVDC Systems

Each DC system has unique characteristics tailored to meet the specific needs of its application. Hence, standard models of fixed structures have not been developed for representation of dc systems in stability studies. The current controller employed in this paper is shown in figure 1. It is a proportional integral controller and the auxiliary controller is assumed to be a constant gain controller.

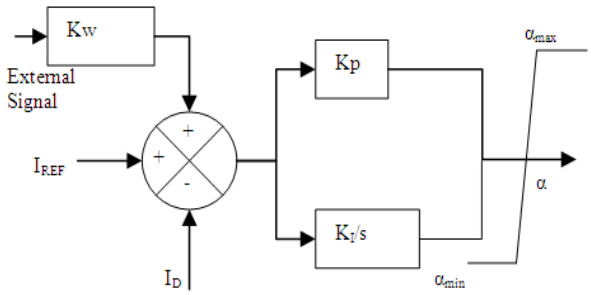

Fig. 1. *Block diagram of current controller*

The HVDC link can be represented as transfer function model [9] as,

$$I_d = \frac{I_{ref}}{1 + sT_d} \quad (15)$$

Where,

Id	dc link current
Iref	reference value of current
Td	Time constant of the system.

3.1. Generator Representation

The synchronous machine is represented by a voltage source, in back of a transient reactance, that is constant in magnitude but changes in angular position neglecting the effect of saliency and assumes constant flux linkages and a small change in speed [10]. The classical generator model

can be described by following set of differential and algebraic equations,

Differential equations,

$$\frac{d\delta}{dt} = \omega - 2\pi f \tag{16}$$

$$\frac{d^2\delta}{dt^2} = \frac{d\omega}{dt} = \frac{\pi f}{H}(P_m - P_e) \tag{17}$$

Algebraic equations,

$$E' = E_t + I_t r_a + j x'_d I_t \tag{18}$$

Where E' Voltage back of transient reactance
E_t Machine terminal voltage
I_t Machine terminal current
r_a Armature resistance
x'_d Transient reactance
δ Rotor angle
ω Speed
P_m, P_e Mechanical and Electrical Power
H Inertia constant

3.2. Load Representation

The static admittance Ypo used to represent the load at bus P, can be obtained from,

$$Y_{po} = \frac{I_{po}}{E_p} \tag{19}$$

4. Steps of AC-DC Transient Stability Study

The basic structure of transient stability program is given below [14]

1. The initial bus voltages are obtained from the ac/dc load flow solution prior to the disturbance.
2. After the ac/dc load flow solution is obtained, the machine currents and voltages behind transient reactance are calculated.
3. The initial speeds and the initial mechanical powers are obtained for each machine prior to the disturbance.
4. The network data is modified for the new representation. Extra nodes are added to represent the generator internal voltages. Admittance matrix is modified to incorporate the load representation.
5. The time is set as t = 0;
6. If there is any switching operation or change in fault condition, the network data is modified accordingly to run the ac/dc load flow.
7. Using Runge-Kutta method, solution of the machine differential equations are obtained to find the changes in the internal voltage angle and machine speeds.
8. Internal voltage angles and machine speeds are updated.
9. Advance time, t = t + Dt.
10. The time limit is to be checked, if t £ t_{max}, then the process has to be repeated from step 6,else the process has to be stopped.

In case of multi machine system stability analysis the relative angles are plotted to evaluate the stability of the power system.

5. Conventional Controller

When a multi machine system is subjected to fault, generator closer to location of fault loses synchronism with the system. To stabilize the system, it is necessary to make equal accelerations of all the generators. So an error signal representing average difference in accelerations of the generators is considered. In case of multi machine system, the relative angles are to be maintained within limits to maintain the stability of the system. So, error signals derived from the average difference in the relative angles and average difference in the relative speeds of the generators are considered.

Considering a 3 machine system and first generator falling out of synchronism, the above mentioned errors can be formulated as below.

$$error_1 = \left[\left(\frac{(\omega(2)-\omega(1))+(\omega(3)-\omega(1))}{2}\right) - (\omega(2)-\omega(3))\right] \tag{20}$$

$$error_2 = \left[\left(\frac{(del(2)-del(1))+(del(3)-del(1))}{2}\right) - (del(2)-del(3))\right] \tag{21}$$

$$error_3 = \left[\left(\frac{\frac{P\_mis(3)}{H(3)}+\frac{P\_mis(2)}{H(2)}}{2}\right) - \left(\frac{P\_mis(1)}{H(1)}\right)\right] \tag{22}$$

Combination of the above three signals are considered, in order to improve the stability. Gains of the signals are varied in order to get better transient and dynamic performance. The signal $error_2$ is equivalent to the integration of the signal $error_1$ and the signal $error_3$ is equivalent to the differentiation of the signal $error_1$. Hence, the controller is equivalent to a PID controller . Then the control signal can be represented as,

$$Error = Kp\, e(t) + Ki\, Ie(t) + Kd\, De(t) \tag{23}$$

$$error = Kp * error1 + Ki * error2 + Kd * error3 \tag{24}$$

6. Neuro – Fuzzy Controller

The structure of the Neuro – Fuzzy controller is shown in figure 2. The recent direction of research is to design a self-organizing fuzzy logic system that has the capability to create the control strategy by learning [11, 12]. The proposed SONFC is a combination of both neural network and fuzzy logic. The fuzzy method provides a structural control framework to express the input-output relationship of the neural network, and the neural network can embed the salient features of computation power and learning capability into the fuzzy controller.

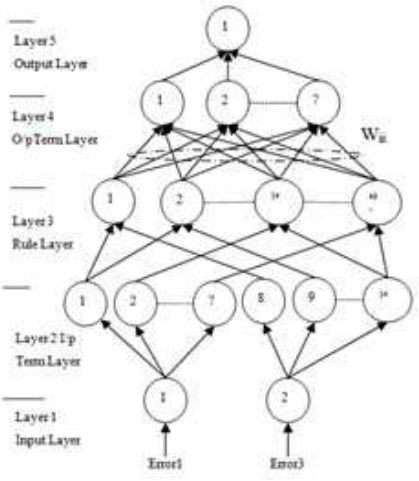

Fig 2. *Topology of Neuro Fuzzy Controller*

6.1. Topology of the Neuro – Fuzzy controller

The proposed NFC is a multilayer neural network-based fuzzy controller. Its overall structure and topology is shown in Fig. 2. The system has a total of five layers. Since two input variables and one output variable are employed in the present work, there are two nodes in layer 1 and one node in layer 5. Nodes in layer 1 are input nodes that directly transmit input signals to the next layer. Layer 5 is the output layer. Nodes in layers 2 and 4 are term nodes that act as membership functions to express the input/output fuzzy linguistic variables. A bell-shaped function is adopted to represent the membership function, in which the mean value m and the variance o will be adapted through the learning process. The fuzzy sets defined for the input/output variables are positive big (PB), positive medium (PM), positive small (PS), zero (ZE), negative small (NS), negative medium (NM), and negative big (NB), which are numbered in descending order in the term nodes. Hence, 14 nodes and 7 nodes are included in layers 2 and 4, respectively, to indicate the input/output linguistic variables. Each node of layer 3 is a rule node that represents one fuzzy control rule. In total, there are 49 nodes in layer 3 to form a fuzzy rule base for two linguistic inputs. Layer 3 links and layer 4 links define the preconditions and consequences of the rule nodes respectively. The NFC adjusts the fuzzy control rules and their membership functions by modifying layer 4 links and the parameters that represent bell – shaped membership function for each node in layer 2 and 4. Following symbols are used to describe various functions:

netiL: the net input value to the i-th node in layer L,

OiL: the output value of the i-th node in layer L,

miL,σiL:the mean and variance of the bell – shaped activation function of the i-th node in layer L,

Wij: the link that connects output layer of j-th node in layer3 with the input to the i-th node in layer 4.

Layer 1: This is a fan – out layer. Inputs are directly transmitted to next layer.

Layer 2: The nodes of this layer act as membership function to express the terms of input linguistic variables.

$$net_i^2 = \begin{cases} O_1^1 & for\ i = 1,2,\ldots.7 \\ O_2^2 & for\ i = 8,9 \ldots 14 \end{cases}$$

$$O_i^2 = e^{-\left(\frac{net_i^2 - m_i^2}{\sigma_i^2}\right)^2} \qquad for\ i = 1,2,\ldots..14 \qquad (25)$$

Note that layer 2 links are all set to unity.

Layer 3: The links in this layer are used to perform precondition matching of fuzzy rules. Thus, each node has two input values from layer 2. The correlation-minimum inference procedure[15] is utilized here to determine the firing strengths of each rule. The output of nodes in this layer is determined by the fuzzy AND operation. Hence, the functions of the layer are given below:

$$net_i^2 = \min\left(O_i^2, O_i^2\right) \qquad (26)$$

The link weights in this layer are also set to unity.

Layer 4: Each node of this layer performs the fuzzy OR operation to integrate the fired rules leading to the same output linguistic variable. Starting with the good initial fuzzy control rules will provide much faster convergence in the learning phase. The functions of this layer are expressed as follows:

$$net_j^4 = \sum_{j=1}^{49} W_{ij} O_j^3 \qquad (27)$$

$$O_j^4 = \min\left(1, net_j^4\right) \qquad for\ j = 1,2 \ldots \ldots 7 \qquad (28)$$

The link weight Wijin this layer expresses the probability of the j-th rule with the i-th output linguistic variable.

Layer5: The node in this layer computes the control signal of the NFC. The output node together with layer 5 links act as a de-fuzzifier. The de-fuzzification aims at producing anon-fuzzy control action that best represents the possibility distribution of an inferred fuzzy control action. The centre of area de-fuzzificationscheme, in which the fuzzy centroidconstitutes the controller output signal, can be simulated.

$$net_1^5 = \sum_{j=1}^{7} m_j^4 \sigma_j^4\, O_j^4 \qquad (29)$$

$$O_j^5 = \frac{net_1^5}{\sum_{j=1}^{7} \sigma_j^4 O_j^4} \qquad (30)$$

6.2. Self-organizing Learning Algorithm

The problem for the self-organized learning can be stated as: Given the training input data xi(t), i = 1, . - . , n , the desired output value yi(t), i = 1,. . . , m ,the fuzzy partitions|T(x)| and |T(y)|, and the desired shapes of membership functions, we want to locate the membership functions and find the fuzzy logic rules. In this phase, the network works in a two-sided manner; that is, the nodes and links at layer four are in the up-down transmission mode so that the training input and output data are fed into this network from both sides. First, the centres (or means) and

the widths (or variances) of the membership functions are determined by self-organized learning techniques analogous to statistical clustering. This serves to allocate network resources efficiently by placing the domains of membership functions covering only those regions of the input/output space where data are present. Kohonen's feature-maps algorithm [20] is adapted here to find the centre mi, of the membership function:

$$\|x(t) - m_{closest}(t)\| = \min_{1\le i\le k}\{\|x(t) - m_i(t)\|\}$$

$$m_{closest}(t+1) = m_{closest}(t) + \propto (t)[x(t) - m_{closest}(t)]$$

$$m_i(t+1) = m_i(t) for\ m_i \neq m_{closest}$$

where *α (t)* is a monotonically decreasing scalar learning rate, and $\boldsymbol{k} = |T(x)|$. This adaptive formulation runs independently for each input and output linguistic variable. The determination of which of the mi's is mclosest can be accomplished in constant time via a winner-take-all circuit. Once the centres of membership functions are found, their widths can be determined by the *N-nearest-neighbors* heuristic by minimizing the following objective function with respect to the widths *(σi's)*

$$\sigma i = \left[\frac{m_i - m_{closest}}{r}\right] \qquad for\ \ i=1,2,....,7 \qquad (31)$$

Then the optimal membership functions and fuzzy rules can be found by gradient – descent search techniques. Thus the energy function is defined as,

$$E = \frac{1}{2}(U^d(k) - U(k))^2 \qquad (7.10)$$

Now using generalized delta rule [14] to minimize the energy, in standard notations, the delta rule can be expressed as,

$$\chi_i(k+1) = \chi_i(k) + \eta\left(-\frac{\partial E}{\partial \chi_i}\right) + \lambda\Delta\chi_i(k) \qquad (7.11)$$

The error signal term delta produced by the i-th neuron in layer L is defined as,

$$\delta_i^L(k) = -\frac{\partial E}{\partial net_i^L} \qquad (7.12)$$

Using above equations, the learning rules of each layer are derived below:

Layer 5: the error signal of the output node is

$$\delta_j^5 = (U^d(k) - U(k) \qquad (7.13)$$

The mean and variance of each output membership function are adapted by,

$$m_i^4(k+1) = m_i^4(k) + \eta\delta_1^5\frac{\sigma_i^4 O_i^4}{\sum_{j=1}^7 \sigma_j^4\, O_j^4} + \lambda\Delta m_i^4(k)$$

$$\sigma_i^4(k+1) = \sigma_i^4(k) + \eta\delta_1^5$$

$$\frac{m_i^4 O_i^4\left(\sum_{j=1}^7 \sigma_j^4\, O_j^4\right) - \sum_{j=1}^7 m_j^4\sigma_j^4\, O_j^4}{\left(\sum_{j=1}^7 \sigma_j^4\, O_j^4\right)^2} + \lambda\Delta\sigma_i^4(k)$$

$$for\ i = 1,2,\dots 7 \qquad (7.14)$$

Layer 4: the error signal of each node is

$$\delta_i^4 = \delta_1^5\frac{m_i^4 O_i^4\left(\sum_{j=1}^7 \sigma_j^4\, O_j^4\right) - \sum_{j=1}^7 m_j^4\sigma_j^4\, O_j^4}{\left(\sum_{j=1}^7 \sigma_j^4\, O_j^4\right)^2}$$

$$for\ i = 1,2,\dots.7; j = 1,2\dots 49$$

The weights between the i-th output linguistic variable and j-th rule is updated by,

$$W_{ij}(k+1) = W_{ij}(k) + \eta\delta_i^4 O_j^3 + \lambda\Delta W_{ij}(k)$$

$$for\ i = 1,2,\dots.7$$

Layer 3: No parameter needs to be adjusted in this layer, and only the error signal needs to be computed and propagated backwards. That is,

$$\delta_i^3 = \sum_{j=1}^7 W_{ij}\,\delta_j^4 \qquad (7.15)$$

Layer 2: The mean and variance of the input membership functions can be updated by,

$$m_i^2(k+1) = m_i^2(k) - \eta\frac{\partial E}{\partial O_i^2}O_i^2\frac{2(O_1^1 - m_i^2)}{(\sigma_i^2)^2} + \propto \Delta m_i^2(k) \qquad (7.16)$$

$$\sigma_i^2(k+1) = \sigma_i^2(k) - \eta\frac{\partial E}{\partial O_i^2}O_i^2\frac{2(O_1^1 - m_i^2)}{(\sigma_i^2)^2} + \propto \Delta\sigma_i^2(k)$$

$$for\ i = 1,2,\dots..14$$

It should be noted that the function of layer 1 is only to distribute the input signal, and hence it is not involved in the learning process. The links connecting layers 4 and 3 can be deleted when the weight is negligibly small or equals zero after learning because it means that this rule node has little or no relationship to the output linguistic variable.

7. Case Study

A WSCC-9 system [13] is taken for stability analysis, it is given in the below figure 4.

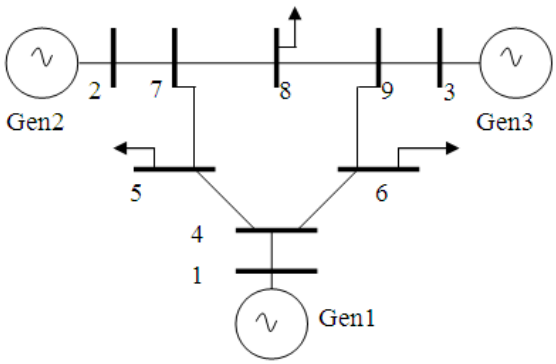

Fig 3. *WSCC 9 bus System*

To test the effectiveness of the above controllers the HVDC system is subjected to a Three-phase-to-ground fault at the converter end AC bus. Variation of dc link voltage and current, and converter firing angle due to a

three-phase-to-ground fault at the rectifier end AC bus. The dc bus voltage completely collapses and results in commutation failure of the converter thyristors. During the fault, the DC link current drops to zero and the firing angle settles at the minimum value. The zero current and zero power condition lead to complete de-energization of the DC link. As soon as the fault is cleared the converter current controller gets activated, and it is in this period when the performance is influenced by the controller actions.

A grounded fault is assumed to occur on Line 4-6, near to Bus 6, at initial time zero and the line from Bus 4 to Bus 6 is removed after 4 cycles. The HVDC line is located between buses 4 –5. Under these conditions, the impact of HVDC on system stability is presented. Initially, a case in which the HVDC line maintains the same control as in the normal state, in which the post-fault HVDC power flow setting remains the same as before, is investigated. It was found that, the system becomes unstable. Then a controller is used to stabilize the system. It is clearly seen from figure 4that the system is becoming unstable, generator 2 and generator 3 are moving together whereas generator 1 falling out of synchronism when no control action is performed.

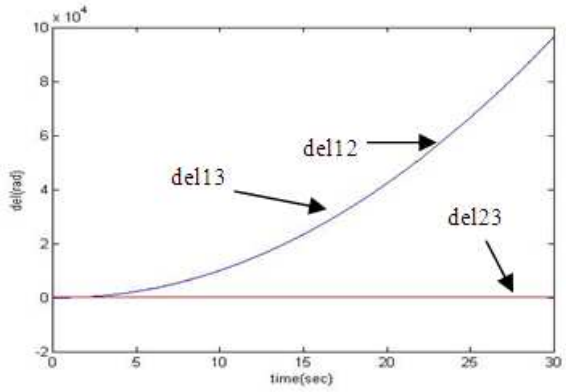

Fig 4. *Plot of relative angles without any external control signal applied*

Different combinations of the three signals in eq. 20, 21, 22 are considered, in order to improve the stability.

Case 1: Considering the signal error3 as the control input, the plot of relative angles is as shown in the fig. 5.

Case 2: Considering the combination of error2 and error3 signals to generate the control signals, the plot of relative angles will be as shown in figure 6.

Case 3: Considering the combination of all the three signals to generate the control signal, the plots of the relative angles with different gains are as shown in fig.7.

Thus from case 3 it is clear that the plot of relative angles of generators can be improved using conventional PID controller. Therefore Fuzzy logic PID controller is also implemented and the plot of relative angles of generators using fuzzy logic controller is shown in fig. 8.

NFC is trained with the available data. Learned Fuzzy Rule matrix using NFC is shown in table 2. The performance of NFC in figures 8,10 is compared with conventional controller and fuzzy logic controller and is summarized in table 3. From table 3, it is clear that proposed NFC works satisfactorily for the given system and gives best results. Similar experiment is done by assuming fault on the line between buses 8 and 9 near bus 8 and the HVDC link is in between buses 4 and 5 and the wave forms are plotted.

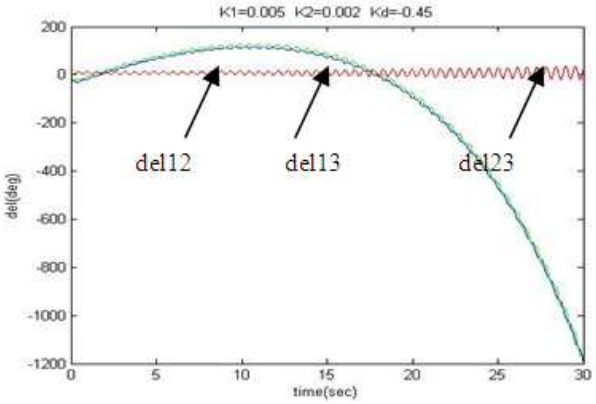

Fig 5. *Plot of relative angles with error$_3$ as the control signal*

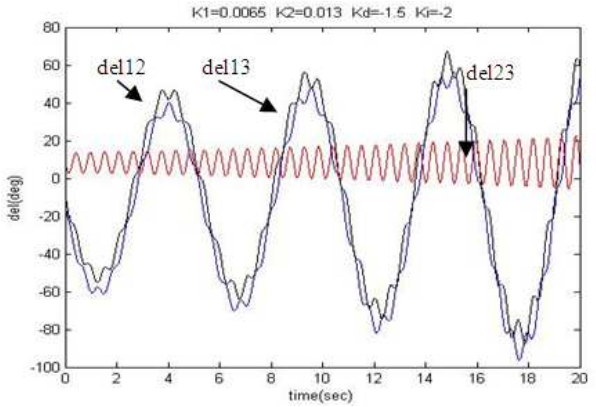

Fig 6. *Plot of relative angles with error$_2$ and error$_3$ as control signals*

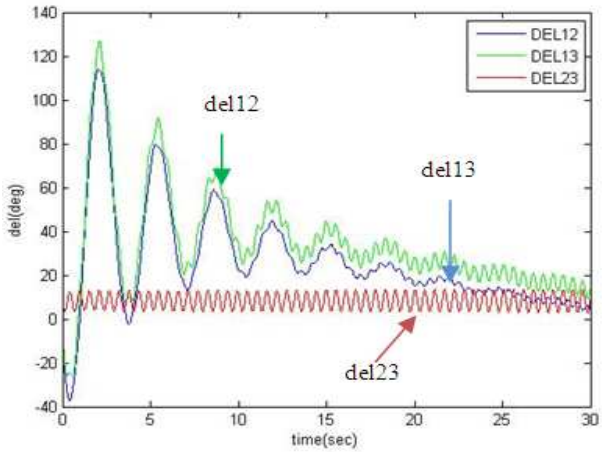

Fig 7. *Plot of relative angles with PID controller. When hvdc link is in between buses 4-5and fault is in between buses 4-6.*

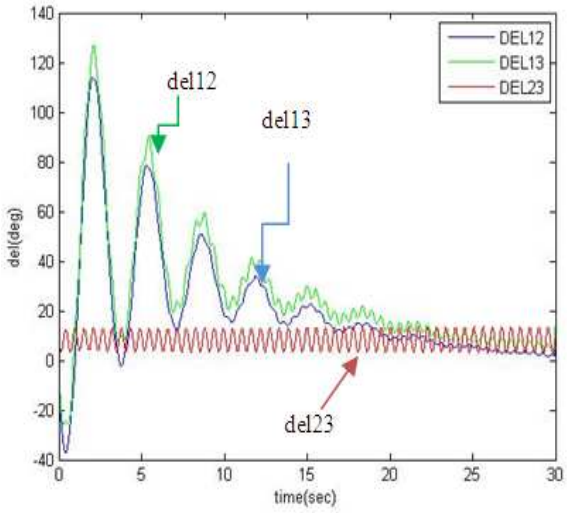

Fig 8. *Plot of relative angles with NeuroFuzzy Controller When hvdc link is in between buses 4-5and fault is in between buses 4-6.*

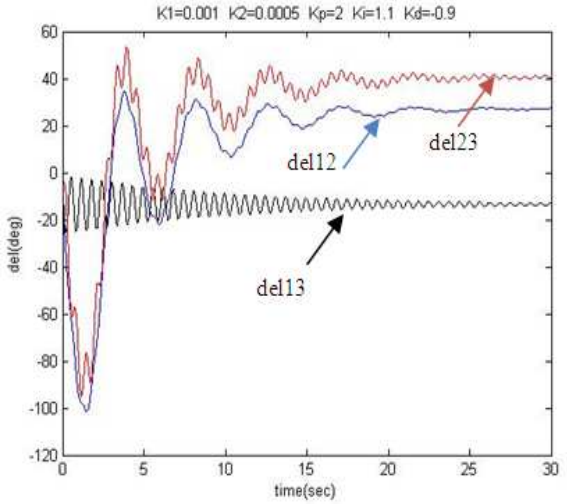

Fig 9. *Plot of relative angles with PID controller. When hvdc link is in between buses 4- 5and ,fault is in between buses 8- 9.*

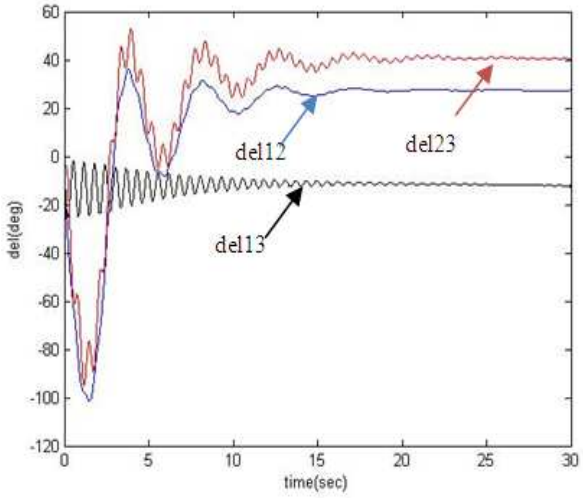

Fig 10. *Plot of relative angles with Neuro-Fuzzy controller. When hvdc link is in between buses 4 and 5,fault is in between buses 8 and 9.*

Table 1. *Initial Fuzzy Rule Matrix*

		Error 1						
		LN	MN	SN	VS	SP	MP	LP
Error3	LP	VS	SP	MP	LP	LP	LP	LP
	MP	SN	VS	SP	MP	MP	LP	LP
	SP	MN	SN	VS	SP	SP	MP	LP
	VS	MN	MN	SN	VS	SP	MP	MP
	SN	LN	MN	SN	SN	VS	SP	MP
	MN	LN	LN	MN	MN	SN	VS	SP
	LN	LN	LN	LN	LN	MN	SN	VS

Table 2. *Learned Fuzzy Rule Matrix*

		Error 1						
		LN	**MN**	**SN**	**VS**	**SP**	**MP**	**LP**
Error3	**LP**				LP			LP
	MP				MP			LP
	SP		LN	MN	SP	LP	LP	LP
	VS	LN	MN	SN	VS	SP	MP	LP
	SN		LN	LN	SN	SN	LP	LP
	MN		LN	LN	MN			
	LN	LN			LN			

Table 3. *Comparison Of Conventional, Fuzzy Logic And Neuro Fuzzy Controller when fault is in between the buses 4 and 6*

Sr. No.	Type of Controller	Generator Controlled	Peak Overshoot	Settling Time
1	Conventional	Gen1	80 deg.	25 sec
2	Fuzzy Logic Based Controller	Gen1	140 deg.	20 sec
3	NFC	Gen1	55 deg.	5 sec

8. Conclusions

Considering the HVDC current controller and line dynamics, it is observed that the transient stability of the multi-machine system is improved only if the combination of all the three signals derived from relative speed (P), rotor angle (D) and average acceleration (I) is used. The paper presents the design of a very simple form of Neuro Fuzzy controller. In this paper, the possibility of replacing a traditional PID controller with a neuro fuzzy controller for the rectifier terminal of an HVDC link is explored.

The neuro fuzzy controller gives better performance than the conventional controller and fuzzy logic controller as expected when compared various aspects of plot of relative angles of the generators such as settling time, peak overshoot etc.

Appendix

Table 4. *Generators Data*

Generator	X_d'	H
1	0.0608	23.64
2	0.1198	6.4
3	0.1813	3.01

Table 5. *Transformers Data*

Transformer	X
1	0.0576
2	0.0625
3	0.0586

Table 6. *Transmission Network Data*

Bus No. P	Bus No. Q	R	X	$y_{pq}/2$
1	4	0.0000	0.0576	0.0000
2	7	0.0000	0.0625	0.0000
3	9	0.0000	0.0586	0.0000
4	6	0.0170	0.0920	0.0790
5	7	0.0320	0.1610	0.1530
6	9	0.0390	0.1700	0.1790
7	8	0.0085	0.0720	0.0745
8	9	0.0119	0.1008	0.1045

Table 7. *Hvdc Line Data*

DC line data		**Initial conditions**	
r_d=0.017, X_c=0.6,	L_d=0.05.	alfa = 0.2094, I_d=0.3691,	P_{di}=0.406
alfamin=5deg, alfamax=80deg		V_{di}=1.1, $P_{M[1]}$=0.756646	gama=0.3142,
taprmin=0.96, taprmax=1.06		$P_{M[2]}$=1.63, $\delta_{M[1]}$=2.388448deg	$P_{M[3]}$=0.85,
tapimin=0.99, tapimax=1.09		$\delta_{M[2]}$=18.603189deg, $\delta_{M[3]}$=12.314856deg	

Table 8. *Generator Data*

Bus No.	P_{GEN}	P_D	Q_D	V_{sp}
1	0.00	0.00	0.00	1.040
2	1.63	0.00	0.00	1.025
3	0.85	0.00	0.00	1.025
4	0.00	0.00	0.00	--
5	0.00	1.25	0.50	--
6	0.00	0.90	0.30	--
7	0.00	0.00	0.00	--
8	0.00	1.00	0.35	--
9	0.00	0.00	0.00	--

References

[1] H. C. Chang and H. C. Chen, "Fast Generation-Shedding Determination in Transient Emergency State," *IEEE Trans. on Energy Conversion, vol. 8, no. 2, pp. 178-183, 1993.*

[2] M. L. Shelton and P. F. Winkelman, "Bonneville Power Administration 1400-MW Brakine Resistor."*IEEE Trans..vol. PAS- 94, pp. 602-609, 1975.*

[3] C.S. Rao and T. K. Nag Sarkar, "Half Wave Thyristor Controlled Dynamic Brake to Improve Transient Stability," *IEEE Trans., vol. PAS-103, no. 5, pp. 1077-1083, May 1984.*

[4] A. Ekstrom and G. Liss, "A refined HVDC control system," *IEEE Trans. Power Apparatus and Systems, vol. PAS-89, no. 536, May/June 1970.*

[5] P. Kundur, *Power System Stability and Control* McGraw-Hill, Inc., 1994

[6] Garng M. Huang, VikramKrishnaswamy, "HVDC Controls for Power System Stability", *IEEE Power Engineering Society, pp 597- 602, 2002.*

[7] V. K. Sood, N. Kandil, R. V. Patel, K. Khorasani, "Comparative Evaluation of Neural-Network-Based and PI Current Controllers for HVDC Transmission", *IEEE Transactions on Power Electronics, VOL.9, NO.3, May1994.*

[8] T. Smed, G. Anderson, "A New Approach to AC/DC Power Flow", *IEEE Trans. on Power Systems., Vol. 6, No. 3, pp 1238- 1244, Aug. 1991.*

[9] K. R. Padiyar,*HVDC Power Transmission Systems* New Age International (P) Ltd., 2004.

[10] Jos Arrillaga and Bruce Smith, "AC- DC Power System Analysis", *The Institution of Electrical Engineers, 1998.*

[11] M. Sugeno and K. Murakami, "Fuzzy Parking control of Model Car,"*in the 13rd IEEE* ***Conf.*** *on Decision and Control,* ***Las*** *Vegas, 1984.*

[12] R. Tauscheit and E. M. Scharf, "Experiments with the Use of a Rule-Based Self-organizing Controller for Robotics Applications," FuzzySets and System, vol. 26, pp. 195-214, 1988.

[13] P.M.Anderson and A.A.Fouad, *Power System Control and Stability*1st ed.,Iowa State University Press, 1977.

[14] Stagg and El- Abiad, *Computer Methods in Power System Analysis* International Student Edition, McGraw- Hill, Book Company, 1968

[15] C. T. Lin and C. **S.** George Lee, "Neural-Network Based Fuzzy LogicControl and Decision System," *IEEE Trans. on Computers, vol. 40,no.12, pp. 1320-1336, Dec. 1991.*